ComEX

IEICE Communications Express, Vol.8, No.3, 73–80

Model-based target classification using polarimetric similarity with coherency matrix elements

Maito Umemura[a)]**, Yoshio Yamaguchi, and Hiroyoshi Yamada**
Graduate School of Science & Technology, Niigata University, 8050 Ikarashi 2-no-cho, Nishi-ku, Niigata 950–2181, Japan
a) *umemura@wave.ie.niigata-u.ac.jp*

Abstract: Polarimetric similarity is a parameter for measuring the similarity between two scattering mechanisms. In this paper, we propose a novel model-based target classification technique using a compensated polarimetric similarity parameter between two coherency matrices. In general, the ensemble average coherency matrix elements have magnitude imbalance, thus the contribution degree to the polarimetric similarity differs for each element. We illustrate how to compensate the contribution degree, and then the proposed method is tested on L-band fully polarimetric ALOS-2/PALSAR-2 data sets by using 4 theoretical scattering models (surface scattering, double-bounce scattering, volume scattering, and 22.5° oriented dihedral scattering). The classification results show that the new compensation scheme serves to better classification.

Keywords: polarimetric synthetic aperture radar, polarimetric similarity, coherency matrix, PolSAR terrain classification
Classification: Sensing

References

[1] A. Freeman and S. L. Durden, "A three-component scattering model for polarimetric SAR data," *IEEE Trans. Geosci. Remote Sens.*, vol. 36, no. 3, pp. 963–973, May 1998. DOI:10.1109/36.673687
[2] Y. Yamaguchi, T. Moriyama, M. Ishido, and H. Yamada, "Four-component scattering model for polarimetric SAR image decomposition," *IEEE Trans. Geosci. Remote Sens.*, vol. 43, no. 8, pp. 1699–1706, Aug. 2005. DOI:10.1109/TGRS.2005.852084
[3] A. Sato, Y. Yamaguchi, G. Singh, and S.-E. Park, "Four-component scattering power decomposition with extended volume scattering model," *IEEE Geosci. Remote Sens. Lett.*, vol. 9, no. 2, pp. 166–170, Mar. 2012. DOI:10.1109/LGRS.2011.2162935
[4] J. Yang, Y. N. Peng, and S. M. Lin, "Similarity between two scattering matrices," *Electron. Lett.*, vol. 37, no. 3, pp. 193–194, Feb. 2001. DOI:10.1049/el:20010104
[5] Q. Chen, Y. M. Jiang, L. J. Zhao, and G. Y. Kuang, "Polarimteric scattering similarity between a random scatterer and a canonical scatterer," *IEEE Geosci. Remote Sens. Lett.*, vol. 7, no. 4, pp. 866–869, Oct. 2010. DOI:10.1109/LGRS.

DOI: 10.1587/comex.2018XBL0152
Received December 10, 2018
Accepted December 28, 2018
Publicized January 21, 2019
Copyedited March 1, 2019

2010.2053912
[6] W. An, W. Zhang, J. Yang, W. Hong, and F. Cao, "On the similarity parameter between two targets for the case of multi-look polarimetric SAR," *Chin. J. Electron.*, vol. 18, pp. 545–550, Jul. 2009.
[7] D. Li and Y. Zhang, "Random similarity between two mixed scatterers," *IEEE Geosci. Remote Sens. Lett.*, vol. 12, no. 12, pp. 2468–2472, Dec. 2015. DOI:10.1109/LGRS.2015.2484383
[8] M. Umemura, Y. Yamaguchi, and H. Yamada, "Model-based target classification using polarimetric similarity with coherency matrix elements," IEICE Tech. Rep., SANE2018-59, Nov. 2018.

1 Introduction

Land cover classification is one of the most important applications of polarimetric synthetic aperture radar (PolSAR) data analysis. In PolSAR data analysis, the ensemble average coherency matrix or covariance matrix are commonly used for deriving the second-order statistics and reducing speckle noise. The scattering power decomposition methods based on the physical theoretical scattering models using the coherency matrix and the covariance matrix have been proposed [1, 2, 3], and those are powerful tool for classifying terrain and retrieving scattering mechanisms. A polarimetric similarity for single-look PolSAR data was first proposed by Yang et al. to measure the similarity between two scattering matrices [4]. It was extended by Chen et al. to measure the similarity between a Pauli scattering vector and a coherency matrix [5]. For the multi-look PolSAR data, a similarity parameter between two coherency matrices have been proposed [6, 7].

However, there is magnitude imbalance in the elements of coherency matrix. Generally, the diagonal elements have large values, whereas off-diagonal elements have small values. If we calculate similarity parameter which needs the inner product operation, the contribution of diagonal elements becomes dominant and the contribution of off-diagonal elements becomes negligible. This means the polarimetric information contained in the off-diagonal terms is lost in the similarity parameter calculation due to the inner product operation [8]. The same is true for the correlation coefficient calculation.

In this paper, we propose a compensation scheme for solving the magnitude imbalance problem and illustrate a model-based target classification technique using the compensated polarimetric similarity parameter. The proposed method is successfully applied to ALOS-2/PALSAR-2 data, showing an excellent classification performance.

2 Polarimetric similarity

From the scattering matrix acquired by the fully PolSAR data sets, the Pauli scattering vector can be created by

$$\boldsymbol{k}_p = \frac{1}{\sqrt{2}}\begin{bmatrix} S_{HH}+S_{VV} \\ S_{HH}-S_{VV} \\ 2S_{HV} \end{bmatrix} \tag{1}$$

DOI: 10.1587/comex.2018XBL0152
Received December 10, 2018
Accepted December 28, 2018
Publicized January 21, 2019
Copyedited March 1, 2019

IEICE Communications Express, Vol.8, No.3, 73–80

where S_{HH}, S_{VV}, and S_{HV} are complex elements of the scattering matrix assuming the backscattering case of $S_{HV} = S_{VH}$.

The ensemble average coherency matrix is expressed by

$$\langle[\boldsymbol{T}]\rangle = \frac{1}{N}\sum^{N} \boldsymbol{k}_p \boldsymbol{k}_p^{\dagger} = \begin{bmatrix} T_{11} & T_{12} & T_{13} \\ T_{21} & T_{22} & T_{23} \\ T_{31} & T_{32} & T_{33} \end{bmatrix} \tag{2}$$

where the superscript † denotes complex conjugate and transpose.

In the coherency matrix, there are 9 (6 real and 3 imaginary) independent elements. Therefore, a vectorized coherency matrix using these independent elements can be expressed as

$$\boldsymbol{T} = [T_{11}\ T_{22}\ T_{33}\ |\mathrm{Re}\{T_{12}\}|\ |\mathrm{Im}\{T_{12}\}|\ |\mathrm{Re}\{T_{13}\}|\ |\mathrm{Im}\{T_{13}\}|\ |\mathrm{Re}\{T_{23}\}|\ |\mathrm{Im}\{T_{23}\}|]^t \tag{3}$$

where the superscript t denotes transpose and $|\cdot|$ denotes absolute value. The absolute value is chosen so that inner product of each element becomes additive.

The polarimetric similarity for measuring the similarity between theoretical scattering model and observed coherency matrix can be defined as

$$\gamma = \frac{\boldsymbol{T_A} \cdot \boldsymbol{T_B}}{\|\boldsymbol{T_A}\|\|\boldsymbol{T_B}\|} \tag{4}$$

where $\cdot$ denotes inner product, $\|\cdot\|$ denotes Euclidean norm, $\boldsymbol{T_A}$ denotes the vectorized coherency matrix of observed data, and $\boldsymbol{T_B}$ denotes vectorized coherency matrix of theoretical scattering model.

3 Compensation scheme

In general, diagonal elements of the ensemble average coherency matrix, namely, T_{11}, T_{22}, and T_{33} have large value as compared with other elements. Hence the degree of contribution to the polarimetric similarity parameter differs for each element. In order to compensate the contribution degree, each element is multiplied by a coefficient as follows:

$$\boldsymbol{T}^{comp} = [aT_{11}\ bT_{22}\ cT_{33}\ d|\mathrm{Re}\{T_{12}\}|\ e|\mathrm{Im}\{T_{12}\}|\ f|\mathrm{Re}\{T_{13}\}|\ g|\mathrm{Im}\{T_{13}\}|\ h|\mathrm{Re}\{T_{23}\}|\ i|\mathrm{Im}\{T_{23}\}|]^t. \tag{5}$$

In order to determine the proper coefficients, we have examined the average absolute value of the coherency matrix elements using 6 data sets (level 1.1, single-look complex) acquired by ALOS-2/PALSAR-2. The examined results of the relative magnitude relation of the coherency matrix elements of the entire images are shown in Table I.

The ID, off-nadir angle, and observation area of data A, B, C, D, E, and F are as follows:

A: ALOS2044980740-150324, 30.4°, San Francisco
B: ALOS2157350670-170422, 30.4°, Los Angeles
C: ALOS2043450820-150313, 30.4°, Barcelona
D: ALOS2035863740-150121, 25°, Amazon
E: ALOS2072670740-150927, 32.7°, Niigata
F: ALOS2066310860-150815, 25°, Hokkaido

DOI: 10.1587/comex.2018XBL0152
Received December 10, 2018
Accepted December 28, 2018
Publicized January 21, 2019
Copyedited March 1, 2019

Table I. Relative magnitude relation of the coherency matrix elements

Data	T_{11}	T_{22}	T_{33}	$\lvert\mathrm{Re}\{T_{12}\}\rvert$	$\lvert\mathrm{Im}\{T_{12}\}\rvert$	$\lvert\mathrm{Re}\{T_{13}\}\rvert$	$\lvert\mathrm{Im}\{T_{13}\}\rvert$	$\lvert\mathrm{Re}\{T_{23}\}\rvert$	$\lvert\mathrm{Im}\{T_{23}\}\rvert$
A	1	0.75	0.25	0.23	0.14	0.07	0.07	0.08	0.05
B	1	0.86	0.26	0.22	0.15	0.08	0.07	0.12	0.05
C	1	0.86	0.26	0.25	0.14	0.09	0.07	0.10	0.04
D	1	0.68	0.47	0.15	0.11	0.08	0.08	0.07	0.07
E	1	0.66	0.23	0.17	0.18	0.07	0.07	0.07	0.04
F	1	0.69	0.24	0.22	0.12	0.06	0.06	0.07	0.04
Avg.	1	0.75	0.29	0.21	0.14	0.08	0.07	0.09	0.05

By checking the values listed in Table I, and by consideration of almost equi-contribution of each element, the magnitude-compensated T vector was chosen as follows,

$$\boldsymbol{T}^{comp} = \Big[T_{11} \ \ \frac{4}{3}T_{22} \ \ 4T_{33} \ \ 5|\mathrm{Re}\{T_{12}\}| \ \ 10|\mathrm{Im}\{T_{12}\}| \\ 10|\mathrm{Re}\{T_{13}\}| \ \ 10|\mathrm{Im}\{T_{13}\}| \ \ 10|\mathrm{Re}\{T_{23}\}| \ \ 10|\mathrm{Im}\{T_{23}\}| \Big]^t. \tag{6}$$

Using Eq. (6), the polarimetric similarity parameter shown in Eq. (4) can be rewritten as

$$\gamma^{comp} = \frac{\boldsymbol{T}_A^{comp} \cdot \boldsymbol{T}_B^{comp}}{\|\boldsymbol{T}_A^{comp}\| \|\boldsymbol{T}_B^{comp}\|}. \tag{7}$$

By measuring the polarimetric similarity between the observed data and the theoretical scattering models using Eq. (7), each multi-looked pixel in the image is classified into a model with best-fit scattering mechanism.

4 Theoretical scattering models

In this paper, we adopt following 4 theoretical scattering models. The surface scattering, double-bounce scattering, and volume scattering model are conventional scattering model proposed in [1, 2]. The 22.5° oriented dihedral scattering model for buildings oriented with respect to radar illumination is derived by modifying probability density function in [3]. Each scattering model is normalized so that the maximum value of elements become unity.

1) Surface scattering:

$$[T]_{surface} = \begin{bmatrix} 1 & \beta^* & 0 \\ \beta & |\beta|^2 & 0 \\ 0 & 0 & 0 \end{bmatrix}. \tag{8}$$

In this paper, we set $\beta = 0.1 + 0.1\mathrm{j}$ as a typical value by data analysis experience.

2) Double-bounce scattering:

DOI: 10.1587/comex.2018XBL0152
Received December 10, 2018
Accepted December 28, 2018
Publicized January 21, 2019
Copyedited March 1, 2019

IEICE Communications Express, Vol.8, No.3, 73–80

$$[T]_{double} = \begin{bmatrix} |\alpha|^2 & \alpha & 0 \\ \alpha^* & 1 & 0 \\ 0 & 0 & 0 \end{bmatrix}. \tag{9}$$

In this paper, we set $\alpha = 0.1 + 0.1\mathrm{j}$.

3) Volume scattering (cloud of randomly oriented dipole):

$$\langle[\boldsymbol{T}]\rangle_{volume} = \begin{bmatrix} 1 & 0 & 0 \\ 0 & \frac{1}{2} & 0 \\ 0 & 0 & \frac{1}{2} \end{bmatrix}. \tag{10}$$

4) 22.5° oriented dihedral corner reflectors scattering:
The scattering matrix of dihedral corner reflector oriented with angle θ can be expressed by

$$[S]_{dihedral(\theta)} = \begin{bmatrix} \cos 2\theta & -\sin 2\theta \\ -\sin 2\theta & -\cos 2\theta \end{bmatrix}. \tag{11}$$

The coherency matrix of the oriented dihedral corner reflector is given by

$$[T]_{dihedral(\theta)} = \begin{bmatrix} 0 & 0 & 0 \\ 0 & \cos^2 2\theta & -\frac{\sin 4\theta}{2} \\ 0 & -\frac{\sin 4\theta}{2} & \sin^2 2\theta \end{bmatrix}. \tag{12}$$

Considering the ensemble averaged data, we adopt a probability density function with its peak at $\pi/8$ as

$$p(\theta) = \frac{1}{2}\cos\left(\theta - \frac{\pi}{8}\right), \quad -\frac{\pi}{2} + \frac{\pi}{8} < \theta < \frac{\pi}{2} + \frac{\pi}{8}. \tag{13}$$

The theoretical ensemble averaged matrix for 22.5° oriented dihedral scattering can be calculated by

$$\langle[T]\rangle_{22.5^\circ\ dihedral} = \int_{-\frac{\pi}{2}+\frac{\pi}{8}}^{\frac{\pi}{2}+\frac{\pi}{8}} [T]_{dihedral(\theta)}\, p(\theta)d\theta. \tag{14}$$

From Eq. (13), the ensemble averaged 22.5° oriented dihedral scattering model can be written as

$$\langle[T]\rangle_{22.5^\circ\ dihedral} = \begin{bmatrix} 0 & 0 & 0 \\ 0 & 1 & \frac{1}{15} \\ 0 & \frac{1}{15} & 1 \end{bmatrix}. \tag{15}$$

5 Classification results

The proposed method is applied to ALOS-2/PALSAR-2 data (level 1.1, single-look complex) over San Francisco, USA, acquired on March 24, 2015. The window size for ensemble average is 6 in the range direction and 12 in the azimuth direction. In all images, the radar illumination direction is from top to bottom.

DOI: 10.1587/comex.2018XBL0152
Received December 10, 2018
Accepted December 28, 2018
Publicized January 21, 2019
Copyedited March 1, 2019

IEICE Communications Express, Vol.8, No.3, 73–80

The classification result before compensating the contribution degree of each coherency matrix element is shown in Fig. 1(a), and the classification result after the compensation is shown in Fig. 1(b). Google Earth image of the same area is shown in Fig. 1(c). Patch A, B, and C are vegetation area, urban buildings area orthogonal to radar illumination, and urban buildings area oriented with respect to radar illumination, respectively.

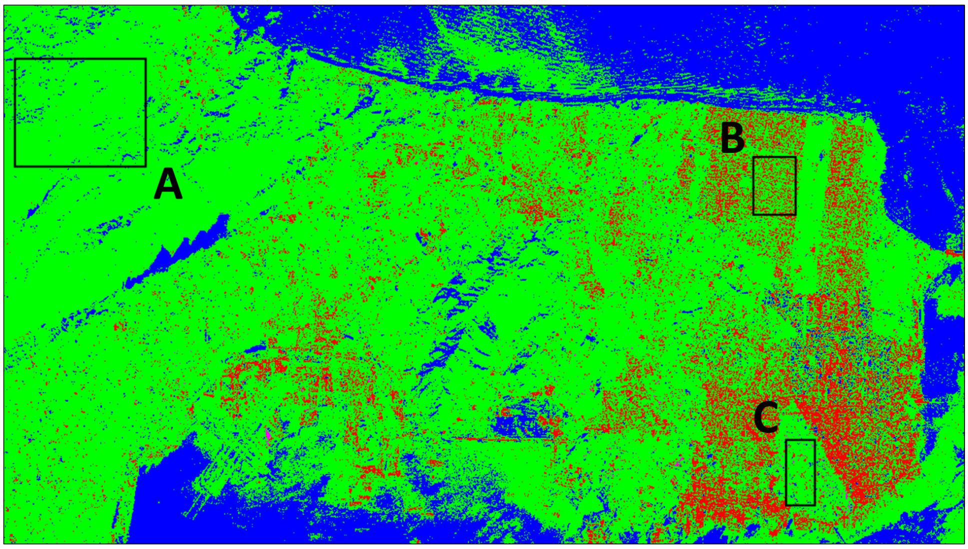

(a) Classification result before the compensation using 4 scattering models (Red : double-bounce scattering, Green : volume scattering, Blue : surface scattering, Magenta : 22.5° oriented dihedral scattering)

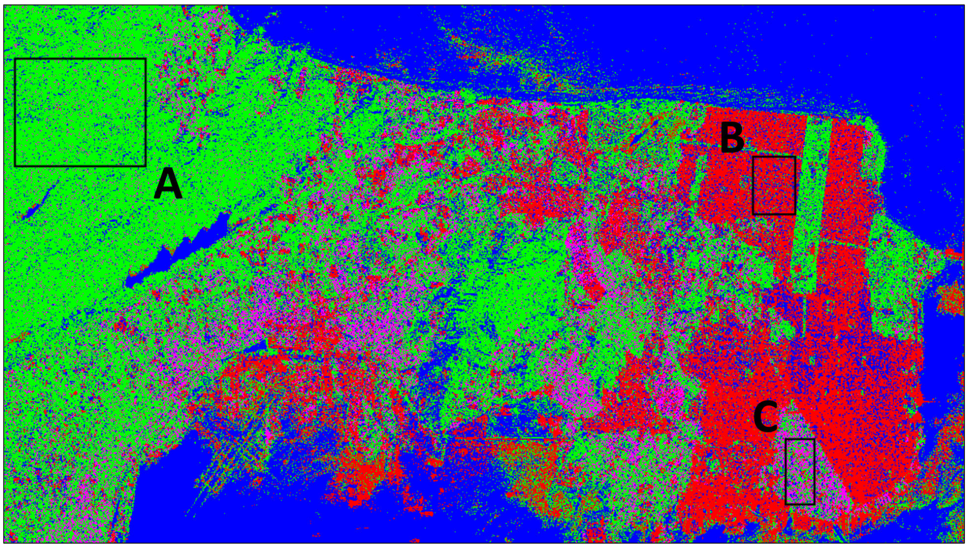

(b) Classification result after the compensation using 4 scattering models (Red : double-bounce scattering, Green : volume scattering, Blue : surface scattering, Magenta : 22.5° oriented dihedral scattering)

DOI: 10.1587/comex.2018XBL0152
Received December 10, 2018
Accepted December 28, 2018
Publicized January 21, 2019
Copyedited March 1, 2019

IEICE Communications Express, Vol.8, No.3, 73–80

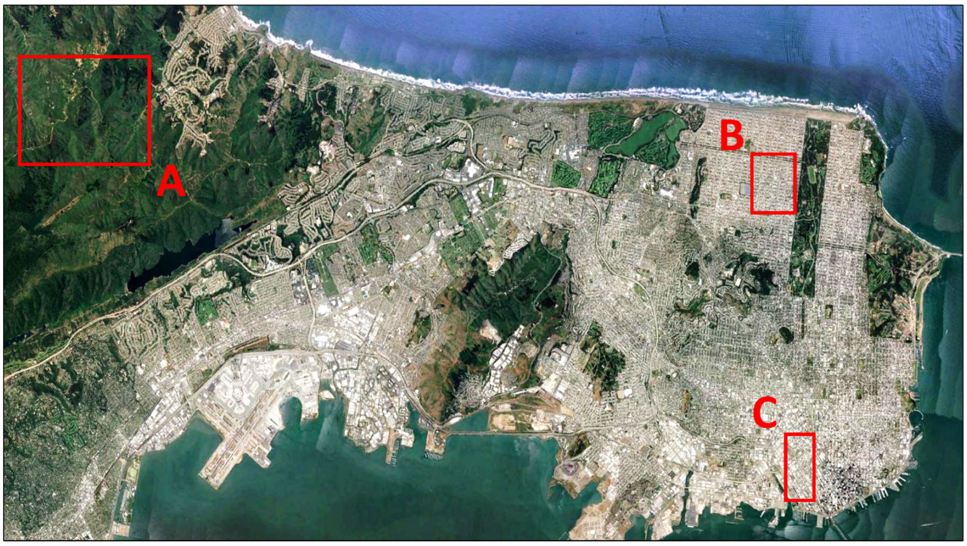

(c) Google Earth image

Fig. 1. Classification results and Google Earth image

From the classification results, it is confirmed that implementation of the compensation scheme is very effective for classification using polarimetric similarity, especially for detecting urban area. In order to evaluate the classification accuracy quantitatively, the classification rates of Patch A, B, and C are shown in Table II.

Table II. Classification rates on typical area

Patch	Surface		Double-bounce		Volume		22.5° oriented dihedral	
	Before [%]	After [%]	Before [%]	After [%]	Before [%]	After [%]	Before [%]	After [%]
A	2.7	6.4	0.0	0.2	97.3	89.1	0.0	4.3
B	0.2	18.7	28.4	75.4	71.4	5.4	0.0	0.5
C	2.4	11.7	4.0	8.3	91.8	36.6	1.8	43.4

For Patch B (orthogonal urban area), 28.4% of pixels are classified into the double-bounce scattering model and 71.4% are classified into the volume scattering model before the compensation scheme. After the compensation, 75.4% are classified into the double-bounce scattering model and 5.4% are classified into the volume scattering model. It is also noticed that the compensation scheme is effective for detecting oriented urban areas. The classification rate of 22.5° oriented dihedral scattering increases from 1.8% to 43.4% by the compensation in oriented urban areas. The classification accuracy in vegetation area is still high as much as 89.1% although in a decreasing tendency. These results are due to the increase of the contribution degrees of T_{12} and T_{23} in orthogonal scattering model and 22.5° oriented dihedral scattering model.

DOI: 10.1587/comex.2018XBL0152
Received December 10, 2018
Accepted December 28, 2018
Publicized January 21, 2019
Copyedited March 1, 2019

6 Conclusion

We have proposed a model-based target classification technique using a compensated polarimetric similarity parameter with the ensemble average coherency matrix elements. The classification results show the new compensation scheme is very effective for model-based classification using polarimetric similarity parameter, especially for detecting urban areas.

Acknowledgments

The authors are grateful to JAXA for providing ALOS-2 data sets under the research contract of RA-6.

DOI: 10.1587/comex.2018XBL0152
Received December 10, 2018
Accepted December 28, 2018
Publicized January 21, 2019
Copyedited March 1, 2019